### Title

Cellular Nanoparticles Treat Coronavirus Infection in Vivo.




### Journal

Nano Letters, 24(47)



### Authors

Yu, Yiyan

Silva-Ayala, Daniela

Zhou, Zhidong

et al.



### Publication Date

2024-11-27

### DOI

10.1021/acs.nanolett.4c04653

Peer reviewed

NANO LETTERS



pubs.acs.org/NanoLett
Letter

# Cellular Nanoparticles Treat Coronavirus Infection *in Vivo*

Yiyan Yu,[†] Daniela Silva-Ayala,[†] Zhidong Zhou, Yifei Peng, Ronnie H. Fang, Weiwei Gao, Anthony Griffiths,* and Liangfang Zhang*

Cite This: *Nano Lett.* 2024, 24, 15136−15141

Read Online

ACCESS | Metrics & More | Article Recommendations | Supporting Information

**ABSTRACT:** Cellular nanoparticles (CNPs), which refer to nanoparticles coated with natural cell membranes, are promising for neutralizing pathological agents. Here, we use CNPs as a medical countermeasure against the infection of SARS-CoV-2 variants in an animal model. CNPs comprise polymeric cores coated with the plasma membranes of human macrophages. The resulting nanoparticles (MΦ-NPs) act as host cell decoys to intercept SARS-CoV-2 and block its cellular entry, thus inhibiting subsequent viral infection. Our findings indicate that MΦ-NPs bind to the spike proteins of SARS-CoV-2 variants in a dose-dependent manner and inhibit the infectivity of live viruses. In hamsters infected with SARS-CoV-2 variants, MΦ-NPs significantly reduce the viral burden in the lungs, demonstrating their effectiveness in inhibiting viral infectivity *in vivo*. Furthermore, MΦ-NPs are primarily taken up by alveolar macrophages without inducing noticeable adverse effects. Given the crucial role of macrophages in viral infections, MΦ-NPs present a promising approach to combating emerging viral threats.

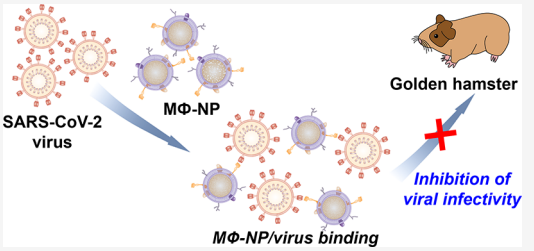


**KEYWORDS:** *cellular nanoparticle, cell membrane coating, biological neutralization, antiviral, coronavirus*

The emergence of new viruses, like the SARS-CoV-2 virus responsible for the COVID-19 pandemic, presents substantial challenges to global health.[1,2] Scientists have been actively researching effective treatments for SARS-CoV-2 infection since its onset.[3,4] Nanotechnology-based approaches, particularly therapeutic nanoparticles, have shown significant potential due to their versatility and multifunctionality.[5,6] For instance, lipid nanoparticles played a crucial role in developing the first approved vaccines against SARS-CoV-2 by delivering mRNA into cells.[7,8] Polymeric nanoparticles have been designed to target antiviral drugs directly to infected cells, reducing off-target effects and minimizing the required dosage.[9,10] Some nanoparticles also offer theranostic capabilities, enabling simultaneous therapeutic intervention and real-time diagnostic monitoring of treatment efficacy.[11,12] Nanoparticles presenting host-binding antigens have effectively blocked SARS-CoV-2 attachment and subsequent infection.[13−16] Inorganic nanoparticles are also promising due to their inherent antiviral properties, including disrupting viral integrity, generating reactive oxygen species, or producing localized heat to deactivate the virus.[17,18] These diverse nanomedicine platforms highlight their promise in combating SARS-CoV-2 infection.

In the past decade, cell membrane-coated nanoparticles (denoted "cellular nanoparticles", or "CNPs") have emerged as a unique biomimetic nanomedicine platform with strong potential for antiviral applications.[19,20] These nanoparticles inherit essential surface antigens from the source cells, allowing them to act as host cell decoys. They bind to viruses and divert them away from their intended host targets, a mechanism that stands apart from conventional antiviral compounds, which require the identification of viral antigens for targeting. This approach addresses the limitation of traditional "one drug−one virus" solutions, which are ineffective against the diverse proteins encoded by different viruses. Since viral infectivity relies on binding with host cell protein receptors, the CNP strategy shifts the focus from the viruses to the hosts, overcoming viral diversity for neutralization. Specific cells, such as T cells or macrophages, are targets of multiple viruses.[21,22] Therefore, CNPs made from the membranes of these cells offer a broad-spectrum neutralization strategy against viral infection. Unlike conventional antiviral treatments that suppress viral replication machinery, CNPs mimic host cell functions for viral neutralization, potentially overcoming viral genetic diversity while avoiding high selective pressure.[23]

The antiviral potential of CNPs was first demonstrated through the inhibition of HIV.[24,25] These CNPs are made with plasma membranes from $CD4^+$ T cells coated onto polymeric cores. They inherited T cell surface antigens critical for HIV binding, effectively neutralizing HIV infectivity. Following the COVID-19 outbreak, researchers developed two types of CNPs from the plasma membranes of human lung epithelial

**Received:** September 20, 2024
**Revised:** November 8, 2024
**Accepted:** November 8, 2024
**Published:** November 13, 2024

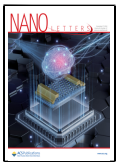

type II cells and human macrophages (MΦs) for neutralizing SARS-CoV-2.[26] These CNPs displayed the same protein receptors as their source cells, which are required for SARS-CoV-2 cellular entry. Upon incubation with the nanosponges, SARS-CoV-2 was neutralized and unable to infect the cells. Further enhancements included increasing the density of surface heparin, a critical viral binding molecule, resulting in a higher capacity of CNPs to neutralize SARS-CoV-2.[16]

To further demonstrate the antiviral potential of CNPs, this study systematically assesses the efficacy of MΦ membrane-coated CNPs (denoted "MΦ-NPs") for treating SARS-CoV-2 infection in an animal model (Figure 1A). Characterization of

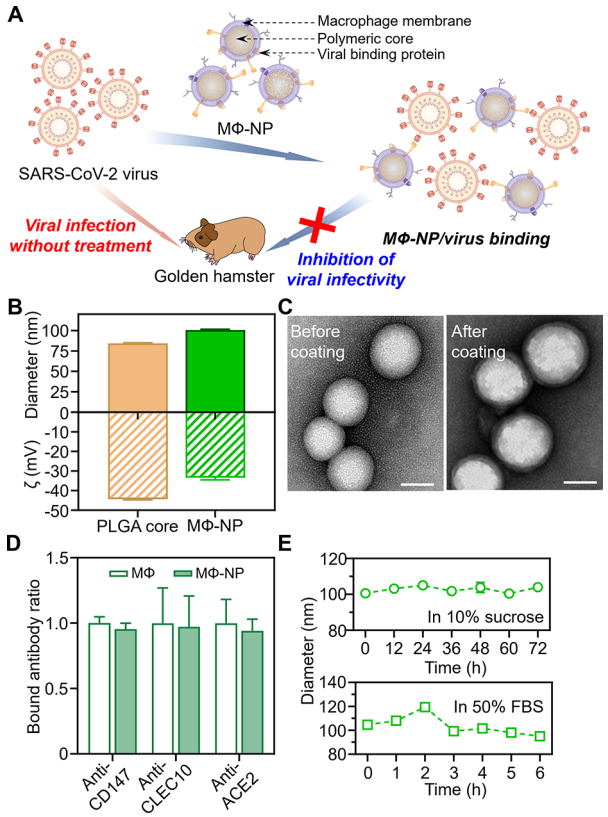


**Figure 1.** Fabrication and physicochemical characterization of MΦ-NPs. (A) Schematic illustration of macrophage-membrane-coated cellular nanoparticles (MΦ-NPs) designed to treat SARS-CoV-2 infection in a hamster model. These MΦ-NPs comprise polymeric cores encased in macrophage-derived membranes, which preserve key membrane proteins essential for virus binding. This interaction effectively inhibits virus−host cell attachment and protects against infection. (B) Size and zeta potential of the MΦ-NPs, determined by dynamic light scattering (DLS). (C) Representative transmission electron microscopy (TEM) image of the PLGA core (left, before coating) and MΦ-NPs (right, after coating). In both images, scale bar = 50 nm. (D) Evaluation of membrane orientation on MΦ-NPs through a comparative analysis of antibody binding between MΦs and MΦ-NPs. (E) Stability assessment of MΦ-NPs in 10% sucrose and 50% fetal bovine serum (FBS).

various physicochemical properties confirmed the successful fabrication of MΦ-NPs. At the protein level, MΦ-NPs effectively bound with the spike (S) proteins of SARS-CoV-2 alpha, beta, and delta strains. At the cellular level, we selected SARS-CoV-2 XBB1.5 and WA strains.[27,28] We demonstrated that MΦ-NPs effectively neutralized live viruses, preventing them from infecting host cells. Using a golden hamster model, we showed that treatment with MΦ-NPs significantly reduced the viral burden in the lungs. Mechanistically, MΦ-NPs were effectively retained in the lungs and were primarily taken up by alveolar macrophages. Moreover, the retention of MΦ-NPs did not induce discernible lung inflammation. These findings suggest that MΦ-NPs have great potential for inhibiting the entry of SARS-CoV-2 variants into host cells and may offer an effective treatment strategy for protecting against SARS-CoV-2 infections.

The synthesis of MΦ-NP consists of three steps. First, using an established differential centrifugation method, we derived the MΦ membrane from THP-1 cells, which are a human monocytic cell line. Second, using a nanoprecipitation method, we synthesized nanoparticle cores with poly(lactic-*co*-glycolic) acid (PLGA). Third, we coated the membrane with the PLGA core through sonication. Before the coating, the hydrodynamic diameter of the nanoparticle core was 84.2 ± 0.8 nm (Figure 1B). After the coating, this value increased to 100.6 ± 1.1 nm, consistent with adding a cell membrane coating to the nanoparticle core. Meanwhile, the surface zeta potential of MΦ-NP (−33.3 ± 1.1 mV) was less negative than that of the noncoated PLGA core (−44.3 ± 0.3 mV). This change in the zeta potential before and after coating indicated charge screening by the cell membrane. The transmission electron microscopy study showed a spherical morphology of the PLGA core before the membrane coating (Figure 1C, left). After being coated, the nanoparticles exhibited a spherical core−shell structure (Figure 1C, right), suggesting the addition of the membrane on the exterior surface. The thickness of the shell was approximately 9 nm, consistent with the typical thickness of a cell membrane.[29]

We also assessed the membrane orientation of the MΦ-NPs by staining ACE2, CLEC10, and CD147 with fluorescently labeled antibodies on MΦ-NPs and MΦs containing equivalent amounts of the membrane material (Figure 1D). The fluorescent intensities measured for each antibody on MΦ-NPs and MΦs were comparable, indicating a right-side-out orientation. An inside-out coating would have made membrane protein receptors inaccessible to the antibodies, reducing fluorescence intensity. Additionally, when the MΦ-NPs were incubated in 10% sucrose for 72 h or in 50% fetal bovine serum (FBS) for 6 h, their diameter showed negligible changes, indicating high colloidal stability (Figure 1E). These results suggest the successful fabrication of MΦ-NPs.

Next, we examined the *in vivo* fate of MΦ-NPs after intratracheal administration. To study lung retention, DiD-labeled MΦ-NPs (25 mg/kg) were administered to mice, and their lungs were collected at predetermined time points for fluorescence measurement. As shown in Figure 2A, the MΦ-NP signal in the lung decreased over time: 87% remained at 6 h, 63% at 24 h, and 30% at 96 h postadministration. Using the Hill equation, we estimated that half of the nanoparticles remained in the lung after 64.3 h, indicating effective lung retention. To evaluate alveolar macrophage (MΦ) uptake of MΦ-NPs, bronchoalveolar lavage (BAL) fluid was collected. Two markers, CD11c and Siglec-F, were stained to identify alveolar MΦs in the BAL fluid, and the percentage of MΦs taking up MΦ-NPs was examined. As shown in Figure 2B, this percentage increased over time following nanoparticle administration and plateaued at 12 h, with approximately 90% of total alveolar MΦs effectively taking up MΦ-NPs. This result suggests that alveolar MΦs mediate the clearance of


https://doi.org/10.1021/acs.nanolett.4c04653
Nano Lett. 2024, 24, 15136−15141

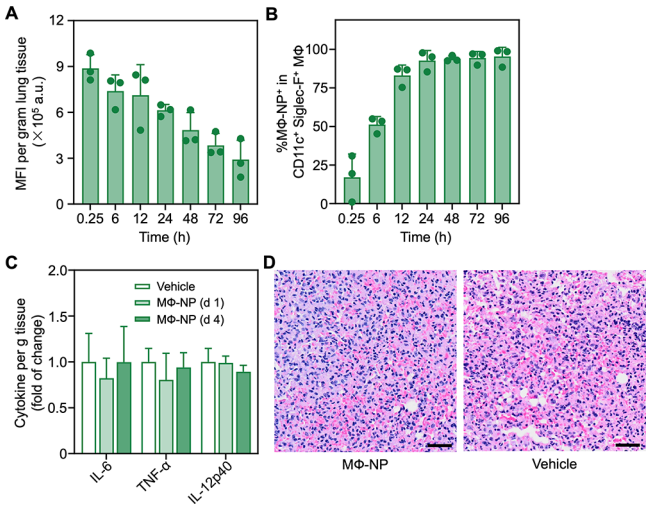


**Figure 2.** Evaluation of MΦ-NP lung retention, uptake by alveolar MΦs, and acute lung toxicity. (A) Lung retention of MΦ-NPs at various time points following intratracheal administration. (B) Flow cytometry analysis quantifying MΦ-NP uptake by CD11c+Siglec-F+ alveolar macrophages at different time points postintratracheal administration. (C) Measurement of lung inflammatory cytokine levels following MΦ-NP instillation. (D) Hematoxylin and eosin (H&E) staining of representative lung sections 96 h after intratracheal administration of MΦ-NPs (scale bar = 50 $\mu$m). In all experiments, $n$ = 3. Panel (A)−(C) data are presented as mean ± s.d.

MΦ-NPs from the lung, which is consistent with previous studies on nanoparticle lung clearance.

We also assessed whether MΦ-NPs caused an acute lung toxicity. MΦ-NPs (25 mg/kg) were administered intratracheally to the mice. On day 1 and day 4 postadministration, mouse lungs were collected to measure the levels of key inflammatory cytokines, including IL-6, TNF-$\alpha$, and IL-12p40. As shown in Figure 2C, cytokine levels in mice receiving the nanoparticles were comparable to those administered with the vehicle, indicating that MΦ-NPs did not induce acute inflammation. Additionally, lung histology was examined at day 4 postadministration. As shown in Figure 2D, hematoxylin and eosin (H&E) stained lung sections from MΦ-NP- and vehicle-treated groups showed comparable morphology, integrity, and immune cell infiltration, suggesting negligible toxicity of MΦ-NPs.

Next, we examined the surface proteins of the MΦ-NPs. First, protein profiles of MΦ lysate, MΦ membrane vesicles, and MΦ-NPs were analyzed by sodium dodecyl sulfate polyacrylamide gel electrophoresis (SDS-PAGE). As shown in Figure 3A, the protein profile of MΦ-NPs was modulated when compared to MΦ lysate (including intracellular proteins) but matched well with that of MΦ membrane vesicles (without intracellular proteins), indicating the preservation of membrane proteins on MΦ-NPs throughout the fabrication process. We next examined the presence of critical viral binding proteins, including ACE2, C-type lectin domain family 10 (CLEC10), and CD147, on the MΦ-NPs.[30,31] Western blot analysis revealed comparable expression levels of these proteins on both the MΦ membrane vesicles and MΦ-NPs, with noticeable enrichment compared to the levels in the MΦ lysate (Figure 3B).

After demonstrating the inheritance of membrane proteins by the MΦ-NPs, we then examined their binding capacity with the receptor-binding domain (RBD) of SARS-CoV-2 spike (S)

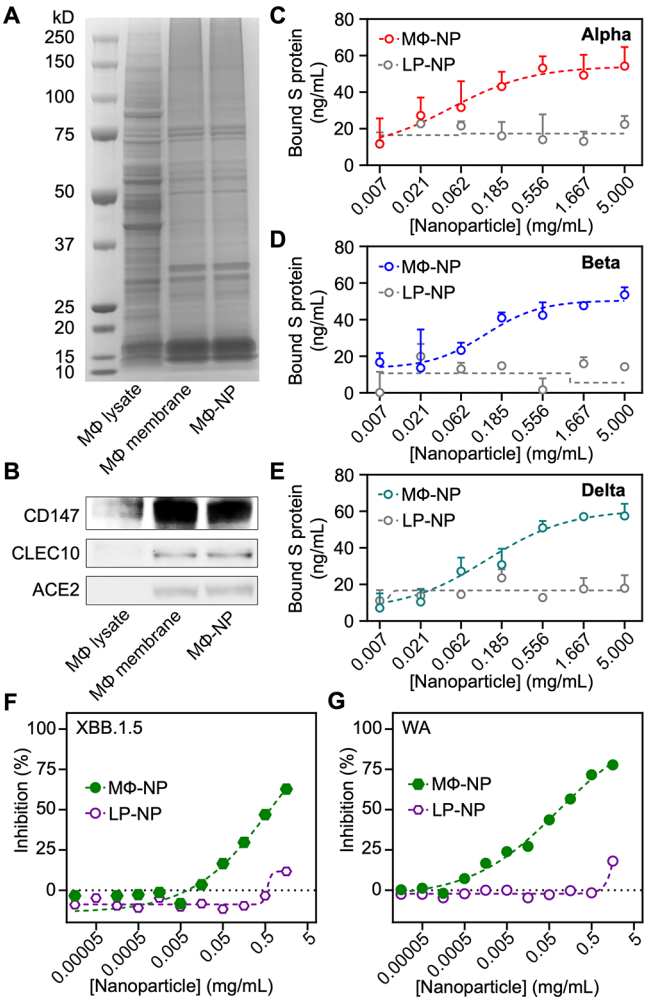


**Figure 3.** Evaluation of MΦ-NPs binding with the spike (S) proteins of various SARS-CoV-2 strains. (A) Protein profiles of MΦ lysate, MΦ membrane vesicles, and MΦ-NPs analyzed via SDS-PAGE. (B) Western blot analysis of selected protein bands from MΦ lysate, MΦ membrane vesicles, and MΦ-NPs. (C−E) Dose-dependent binding profiles of MΦ-NPs with the spike proteins of different SARS-CoV-2 variants: (C) Alpha, (D) Beta, and (E) Delta strains. (F, G) MΦ-NPs neutralize the infectivity of live SARS-CoV-2 (F) XBB.1.5 strain and (G) the WA strain, respectively ($n$ = 6). Dose-dependent neutralization profiles indicate the efficacy. The study used lipid−polymer hybrid nanoparticles (LP-NPs) as the control group.

proteins. The initial test was conducted with RBD proteins from the SARS-CoV-2 alpha strain. As shown in Figure 3C, as the concentration of MΦ-NPs increased, the amount of bound RBD protein also increased, exhibiting dose-dependent binding with a typical sigmoidal profile. Based on this measurement, the half-maximal inhibitory concentration ($IC_{50}$) of MΦ-NPs was 0.05 ± 0.01 mg/mL. In contrast, the lipid−polymer hybrid nanoparticles (denoted "LP-NPs") used as a control showed negligible binding with the RBD protein, confirming the binding specificity between MΦ-NPs and the RBD proteins. Binding studies were also conducted using RBD proteins from the SARS-CoV-2 beta and delta strains. The binding of MΦ-NPs with these proteins exhibited similar sigmoidal profiles (Figures 3D and 3E). The $IC_{50}$ values were calculated as 0.12 ± 0.02 and 0.12 ± 0.10 mg/mL for the beta and delta strains, respectively.


https://doi.org/10.1021/acs.nanolett.4c04653
Nano Lett. 2024, 24, 15136−15141

We further examined the capability of MΦ-NPs in neutralizing the infectivity of live SARS-CoV-2 viruses by a plaque reduction neutralization test. In the study, a low passage sample of SARS-CoV-2 (XBB.1.5) was amplified in Vero E6 cells to make a working stock of the virus. Serial log dilutions of the MΦ-NPs were mixed with SARS-CoV-2, followed by testing of viral infectivity. As shown in Figure 3F, inhibition of the infectivity increased as the concentration of MΦ-NPs increased, suggesting a dose-dependent neutralization effect. Based on the results, an $IC_{50}$ value of 0.68 ± 0.02 μg/mL was obtained. In parallel, a similar dose-dependent inhibition of viral infectivity was observed with the WA strain (Figure 3G). An $IC_{50}$ value of 0.08 ± 0.02 μg/mL was obtained in this case. In both experiments, LP-NP control nanoparticles were also tested in parallel for viral inhibition. The control nanoparticles were ineffective in neutralizing either SARS-CoV-2 strain, confirming that the inhibition was due to the macrophage membrane coating.

Following the *in vitro* testing, we next evaluated the efficacy of MΦ-NP in neutralizing SARS-CoV-2 in Syrian golden hamsters.[32,33] In the study, MΦ-NPs were administered intratracheally, and the animals were then challenged with the SARS-CoV-2 XBB.1.5 strain through intranasal inoculation 6 h after MΦ-NP administration. We assessed efficacy by measuring the viral burden in the lungs 4 days postinfection. Compared with hamsters receiving the vehicle or LP-NPs, those treated with MΦ-NPs exhibited the lowest viral burden, indicating the effectiveness of MΦ-NPs (Figure 4A). Similar results were observed when challenging the hamsters with the WA strain. As shown in Figure 4B, the MΦ-NP-treated group exhibited the lowest viral burden in the lungs. These results demonstrate that MΦ-NPs effectively neutralize SARS-CoV-2 variants in hamsters.

The efficacy of the MΦ-NP treatment was further confirmed using a subgenomic RT-qPCR assay targeting the SARS-CoV-2 E gene, which indicates active viral replication. In hamsters infected with the XBB.1.5 strain, viral RNA levels at 4 days postinfection were approximately $10^8$ RNA copies per gram of tissue in both the vehicle and LP-NP groups (Figure 4C). In contrast, hamsters treated with MΦ-NPs exhibited a 100,000-fold reduction in viral RNA levels. A similar level of efficacy was observed in hamsters infected with the WA strain (Figure 4D). Additionally, the expression levels of inflammatory markers, including MIP-1α, MCP-1, and IL-10, were measured in the lung tissues of hamsters infected with either the XBB.1.5 or WA strains (Figure 4E,F). In both groups, a significant increase in the expression levels of these markers was observed in hamsters treated with the vehicle or LP-NPs. Conversely, hamsters treated with MΦ-NPs showed significantly lower expression levels of these markers. These results further confirm the protective effect of MΦ-NPs against SARS-CoV-2 infection *in vivo*.

In summary, we developed MΦ-NPs by coating polymeric cores with human macrophage membranes and demonstrated their broad-spectrum antiviral capabilities against SARS-CoV-2 variants. MΦ-NPs were stable in buffer solutions and possessed antigens that were crucial for viral entry. We showed that MΦ-NPs bound to the spike proteins of the SARS-CoV-2 alpha, beta, and delta variants. *In vitro*, MΦ-NPs effectively blocked the cellular entry of SARS-CoV-2. *In vivo*, treatment with MΦ-NPs in golden hamsters infected with SARS-CoV-2 variants inhibited viral infection, as evidenced by the reduced viral burden in the animals. Importantly, MΦ-NPs were

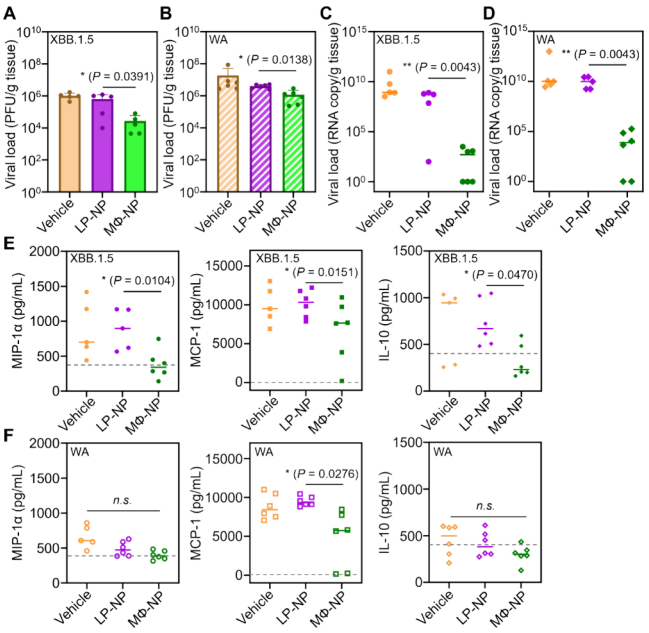


**Figure 4.** MΦ-NPs neutralize SARS-CoV-2 *in vivo*. (A, B) Lung viral load in hamsters infected with SARS-CoV-2 (A) XBB.1.5 ($n$ = 5) and (B) WA strains ($n$ = 6), respectively, and treated with MΦ-NPs. The vehicle (10% sucrose) and the LP-NPs were used as two controls in the study. (C, D) Viral load in the lung tissue of hamsters infected with SARS-CoV-2 (C) XBB.1.5 and (D) WA strains, quantified with a subgenomic RT-qPCR assay targeting the E gene of SARS-CoV-2. (E, F) Levels of MIP-1α, MCP-1, and IL-10 in lung tissues of hamsters infected with (E) XBB.1.5 and (F) WA strains, respectively. The dashed line represents the cytokine baseline measured from healthy animals. Statistical analysis was performed using a paired two-tailed $t$-test. Data presented as mean ± s.d. Statistical comparisons are indicated by '*': * for $P < 0.05$, ** for $P < 0.01$, *** for $P < 0.001$;.

predominantly taken up by alveolar macrophages without causing noticeable inflammation in the lungs, indicating a high safety threshold. Overall, these findings show MΦ-NPs as a promising broad-spectrum antiviral platform for treating various SARS-CoV-2 variants.

In this study, we selected human macrophage membranes due to their relevance for future clinical translation to humans. Using human macrophage membranes in hamsters may potentially trigger an immune response. However, as MΦ-NPs are nonliving, they do not amplify the immune response but rather undergo faster clearance, which could reduce their efficacy. The significant effectiveness of human MΦ-NPs observed in hamsters suggests their high potential for future use in humans. In addition, macrophages have M1 and M2 polarization states, but the present study used the THP-1 cell line that was not polarized.

In our investigation, MΦ-NPs function as cellular decoys that bind to viruses, effectively blocking viral entry. Given the complex roles of macrophages in viral infections, this binding may also inhibit various signaling processes, resulting in faster viral clearance, more efficient inflammation resolution, and better suppression against viral replication or virion release.[34,35] Unraveling these mechanisms will enrich our understanding of the biointerfacial properties of cellular nanoparticles. Furthermore, nanoparticle−virus complexes formed *in situ* may stimulate an antiviral immune response, contributing to a meaningful antiviral immunity. Previous studies have shown that complexes formed between nano-


https://doi.org/10.1021/acs.nanolett.4c04653
Nano Lett. 2024, 24, 15136−15141

particles and viruses or viral components can elicit effective antiviral responses.[36,37] Additionally, nanoparticles that capture bacterial components *in situ* have demonstrated success in generating antibacterial immunity.[38] This *in situ* immunization approach holds exciting potential for antiviral vaccine design, opening new avenues for research and enhancing antiviral effectiveness. Given these potentials of MΦ-NPs, we expect that they can be an effective approach for the treatment of other respiratory viral infections.

## ■ ASSOCIATED CONTENT

### Supporting Information

The Supporting Information is available free of charge at https://pubs.acs.org/doi/10.1021/acs.nanolett.4c04653.

Additional experimental details, materials, and methods, including cell membrane derivation, MΦ-NP and LP-NP fabrication, MΦ-NP characterization, membrane sidedness study, MΦ-NP lung retention and uptake by alveolar MΦs, *in vivo* safety studies, membrane protein characterization using SDS-PAGE and Western blotting, MΦ-NP binding with S-RBD proteins of SARS-CoV-2, virus information, plaque reduction neutralization assay, evaluation of MΦ-NP against SARS-CoV-2 in Syrian golden hamsters, lung tissue viral load quantification, quantitative RT-qPCR SARS-CoV-2 subgenomic RNA viral load, and multiplex cytokine analysis (PDF)

## ■ AUTHOR INFORMATION


### Corresponding Authors

**Anthony Griffiths** − *Department of Microbiology and National Emerging Infectious Diseases Laboratories, School of Medicine, Boston University, Boston, Massachusetts 02115, United States; Laboratory for Infectious Disease Research and Department of Molecular Microbiology and Immunology, School of Medicine, University of Missouri, Columbia, Missouri 65211, United States*; Email: agriffiths@missouri.edu

**Liangfang Zhang** − *Aiiso Yufeng Li Family Department of Chemical and Nano Engineering, Shu and K.C. Chien and Peter Farrell Collaboratory, University of California San Diego, La Jolla, California 92093, United States;* orcid.org/0000-0003-0637-0654; Email: zhang@ucsd.edu

### Authors

**Yiyan Yu** − *Aiiso Yufeng Li Family Department of Chemical and Nano Engineering, Shu and K.C. Chien and Peter Farrell Collaboratory, University of California San Diego, La Jolla, California 92093, United States;* orcid.org/0000-0002-7136-654X

**Daniela Silva-Ayala** − *Department of Microbiology and National Emerging Infectious Diseases Laboratories, School of Medicine, Boston University, Boston, Massachusetts 02115, United States*

**Zhidong Zhou** − *Aiiso Yufeng Li Family Department of Chemical and Nano Engineering, Shu and K.C. Chien and Peter Farrell Collaboratory, University of California San Diego, La Jolla, California 92093, United States*

**Yifei Peng** − *Aiiso Yufeng Li Family Department of Chemical and Nano Engineering, Shu and K.C. Chien and Peter Farrell Collaboratory, University of California San Diego, La Jolla, California 92093, United States*

**Ronnie H. Fang** − *Aiiso Yufeng Li Family Department of Chemical and Nano Engineering, Shu and K.C. Chien and Peter Farrell Collaboratory, University of California San Diego, La Jolla, California 92093, United States;* orcid.org/0000-0001-6373-3189

**Weiwei Gao** − *Aiiso Yufeng Li Family Department of Chemical and Nano Engineering, Shu and K.C. Chien and Peter Farrell Collaboratory, University of California San Diego, La Jolla, California 92093, United States;* orcid.org/0000-0001-5196-4887

Complete contact information is available at: https://pubs.acs.org/10.1021/acs.nanolett.4c04653


### Author Contributions

†Y.Y. and D.S.-A. contributed equally to this work. Y.Y., D.S-A., W.G., A.G., and L.Z. designed the study. Y.Y., D.S-A., Z.Z., and Y.P. performed the experiments. Y.Y., D.S-A., R.H.F., and W.G. analyzed the data. Y.Y., D.S-A., R.H.F., W.G., A.G., and L.Z. wrote the paper.

### Notes

The authors declare the following competing financial interest(s): L.Z. discloses financial interest in Cellics Therapeutics. All other authors declare no competing interests.

## ■ ACKNOWLEDGMENTS

This work was supported by the Department of Defense, Defense Threat Reduction Agency, under award number HDTRA1-21-C-0019. The content of the information does not necessarily reflect the position or the policy of the federal government, and no official endorsement should be inferred.

## ■ REFERENCES


(1) Sohrabi, C.; Alsafi, Z.; O'Neill, N.; Khan, M.; Kerwan, A.; Al-Jabir, A.; Iosifidis, C.; Agha, R. World Health Organization declares global emergency: A review of the 2019 novel coronavirus (COVID-19). *Int. J. Surg.* **2020**, *76*, 71−76.

(2) Wang, C.; Horby, P. W.; Hayden, F. G.; Gao, G. F. A novel coronavirus outbreak of global health concern. *Lancet* **2020**, *395*, 470−473.

(3) Li, G. D.; Hilgenfeld, R.; Whitley, R.; De Clercq, E. Therapeutic strategies for COVID-19: progress and lessons learned. *Nat. Rev. Drug Discovery* **2023**, *22*, 449−475.

(4) Murakami, N.; Hayden, R.; Hills, T.; Al-Samkari, H.; Casey, J.; Del Sorbo, L.; Lawler, P. R.; Sise, M. E.; Leaf, D. E. Therapeutic advances in COVID-19. *Nat. Rev. Nephrol.* **2023**, *19*, 38−52.

(5) Huang, X. G.; Kon, E.; Han, X. X.; Zhang, X. C.; Kong, N.; Mitchell, M. J.; Peer, D.; Tao, W. Nanotechnology-based strategies against SARS-CoV-2 variants. *Nat. Nanotechnol.* **2022**, *17*, 1027−1037.

(6) Duan, Y.; Wang, S. Y.; Zhang, Q. Z.; Gao, W.; Zhang, L. Nanoparticle approaches against SARS-CoV-2 infection. *Curr. Opin. Solid State Mater. Sci.* **2021**, *25*, 100964.

(7) Creech, C. B.; Walker, S. C.; Samuels, R. J. SARS-CoV-2 Vaccines. *J. Am. Med. Assoc.* **2021**, *325*, 1318−1320.

(8) Krause, P. R.; Fleming, T. R.; Longini, I. M.; Peto, R.; Briand, S.; Heymann, D. L.; Beral, V.; Snape, M. D.; Rees, H.; Ropero, A. M.; et al. SARS-CoV-2 Variants and Vaccines. *N. Engl. J. Med.* **2021**, *385*, 179−186.

(9) Sanna, V.; Satta, S.; Hsiai, T.; Sechi, M. Development of targeted nanoparticles loaded with antiviral drugs for SARS-CoV-2 inhibition. *Eur. J. Med. Chem.* **2022**, *231*, 114121.

(10) Beach, M. A.; Nayanathara, U.; Gao, Y. T.; Zhang, C. H.; Xiong, Y. J.; Wang, Y. F.; Such, G. K. Polymeric Nanoparticles for Drug Delivery. *Chem. Rev.* **2024**, *124*, 5505−5616.

(11) Dhar, A.; Gupta, S. L.; Saini, P.; Sinha, K.; Khandelwal, A.; Tyagi, R.; Singh, A.; Sharma, P.; Jaiswal, R. K. Nanotechnology-based theranostic and prophylactic approaches against SARS-CoV-2. *Immunol. Res.* **2024**, *72*, 14−33.
(12) Itani, R.; Tobaiqy, M.; Al Faraj, A. Optimizing use of theranostic nanoparticles as a life-saving strategy for treating COVID-19 patients. *Theranostics* **2020**, *10*, 5932−5942.
(13) Yang, Z. Q.; Hua, L. Q.; Yang, M. L.; Liu, S. Q.; Shen, J. X.; Li, W. R.; Long, Q.; Bai, H. M.; Yang, X.; Ren, Z. L.; et al. RBD-Modified Bacterial Vesicles Elicited Potential Protective Immunity against SARS-CoV-2. *Nano Lett.* **2021**, *21*, 5920−5930.
(14) Wang, Z. Z.; Popowski, K. D.; Zhu, D. S.; Abad, B. L. D.; Wang, X. Y.; Liu, M. R.; Lutz, H.; De Naeyer, N.; DeMarco, C. T.; Denny, T. N.; et al. Exosomes decorated with a recombinant SARS-CoV-2 receptor-binding domain as an inhalable COVID-19 vaccine. *Nat. Biomed. Eng.* **2022**, *6*, 791−805.
(15) Rao, L.; Xia, S.; Xu, W.; Tian, R.; Yu, G. C.; Gu, C. J.; Pan, P.; Meng, Q. F.; Cai, X.; Qu, D.; et al. Decoy nanoparticles protect against COVID-19 by concurrently adsorbing viruses and inflammatory cytokines. *Proc. Natl. Acad. Sci. U. S. A.* **2020**, *117*, 27141−27147.
(16) Ai, X. Z.; Wang, D.; Honko, A.; Duan, Y. O.; Gavrish, I.; Fang, R. H.; Griffiths, A.; Gao, W.; Zhang, L. Surface Glycan Modification of Cellular Nanosponges to Promote SARS-CoV-2 Inhibition. *J. Am. Chem. Soc.* **2021**, *143*, 17615−17621.
(17) Zhou, Y. Y.; Fletcher, N. F.; Zhang, N.; Hassan, J.; Gilchrist, M. D. Enhancement of Antiviral Effect of Plastic Film against SARS-CoV-2: Combining Nanomaterials and Nanopatterns with Scalability for Mass Manufacturing. *Nano Lett.* **2021**, *21*, 10149−10156.
(18) Jeremiah, S. S.; Miyakawa, K.; Morita, T.; Yamaoka, Y.; Ryo, A. Potent antiviral effect of silver nanoparticles on SARS-CoV-2. *Biochem. Biophys. Res. Commun.* **2020**, *533*, 195−200.
(19) Fang, R. H.; Kroll, A. V.; Gao, W.; Zhang, L. Cell Membrane Coating Nanotechnology. *Adv. Mater.* **2018**, *30*, 1706759.
(20) Wang, S. Y.; Wang, D.; Duan, Y. O.; Zhou, Z. D.; Gao, W.; Zhang, L. Cellular Nanosponges for Biological Neutralization. *Adv. Mater.* **2022**, *34*, 2107719.
(21) Moss, P. The T cell immune response against SARS-CoV-2. *Nat. Immunol.* **2022**, *23*, 186−193.
(22) Abassi, Z.; Knaney, Y.; Karram, T.; Heyman, S. N. The Lung Macrophage in SARS-CoV-2 Infection: A Friend or a Foe? *Front. Immunol.* **2020**, *11*, 1312.
(23) Hirotsu, Y.; Kobayashi, H.; Kakizaki, Y.; Saito, A.; Tsutsui, T.; Kawaguchi, M.; Shimamura, S.; Hata, K.; Hanawa, S.; Toyama, J.; et al. Multidrug-resistant mutations to antiviral and antibody therapy in an immunocompromised patient infected with SARS-CoV-2. *Med.* **2023**, *4*, 813−824.
(24) Wei, X. L.; Zhang, G.; Ran, D. N.; Krishnan, N.; Fang, R. H.; Gao, W.; Spector, S. A.; Zhang, L. T-Cell-Mimicking Nanoparticles Can. Neutralize HIV Infectivity. *Adv. Mater.* **2018**, *30*, 1802233.
(25) Zhang, G.; Campbell, G. R.; Zhang, Q. Z.; Maule, E.; Hanna, J.; Gao, W.; Zhang, L.; Spector, S. A. CD4+ T Cell-Mimicking Nanoparticles Broadly Neutralize HIV-1 and Suppress Viral Replication through Autophagy. *Mbio* **2020**, *11*, No. e00903-20.
(26) Zhang, Q. Z.; Honko, A.; Zhou, J. R.; Gong, H.; Downs, S. N.; Vasquez, J. H.; Fang, R. H.; Gao, W.; Griffiths, A.; Zhang, L. Cellular Nanosponges Inhibit SARS-CoV-2 Infectivity. *Nano Lett.* **2020**, *20*, 5570−5574.
(27) Tamura, T.; Irie, T.; Deguchi, S.; Yajima, H.; Tsuda, M.; Nasser, H.; Mizuma, K.; Plianchaisuk, A.; Suzuki, S.; Uriu, K.; et al. Virological characteristics of the SARS-CoV-2 Omicron XBB.1.5 variant. *Nat. Commun.* **2024**, *15*, 1176.
(28) Paredes, M. I.; Lunn, S. M.; Famulare, M.; Frisbie, L. A.; Painter, I.; Burstein, R.; Roychoudhury, P.; Xie, H.; Bakhash, S. A. M.; Perez, R.; et al. Associations Between Severe Acute Respiratory Syndrome Coronavirus 2 (SARS-CoV-2) Variants and Risk of Coronavirus Disease 2019 (COVID-19) Hospitalization Among Confirmed Cases in Washington State: A Retrospective Cohort Study. *Clin. Infect. Dis.* **2022**, *75*, No. E536-E544.
(29) Hu, C. M. J.; Zhang, L.; Aryal, S.; Cheung, C.; Fang, R. H.; Zhang, L. Erythrocyte membrane-camouflaged polymeric nanoparticles as a biomimetic delivery platform. *Proc. Natl. Acad. Sci. U. S. A.* **2011**, *108*, 10980−10985.
(30) Fenizia, C.; Galbiati, S.; Vanetti, C.; Vago, R.; Clerici, M.; Tacchetti, C.; Daniele, T. SARS-CoV-2 Entry: At the Crossroads of CD147 and ACE2. *Cells* **2021**, *10*, 1434.
(31) Lempp, F. A.; Soriaga, L. B.; Montiel-Ruiz, M.; Benigni, F.; Noack, J.; Park, Y. J.; Bianchi, S.; Walls, A. C.; Bowen, J. E.; Zhou, J. Y.; et al. Lectins enhance SARS-CoV-2 infection and influence neutralizing antibodies. *Nature* **2021**, *598*, 342−347.
(32) Imai, M.; Iwatsuki-Horimoto, K.; Hatta, M.; Loeber, S.; Halfmann, P. J.; Nakajima, N.; Watanabe, T.; Ujie, M.; Takahashi, K.; Ito, M.; et al. Syrian hamsters as a small animal model for SARS-CoV-2 infection and countermeasure development. *Proc. Natl. Acad. Sci. U. S. A.* **2020**, *117*, 16587−16595.
(33) Rogers, T. F.; Zhao, F. Z.; Huang, D. L.; Beutler, N.; Burns, A.; He, W. T.; Limbo, O.; Smith, C.; Song, G.; Woehl, J.; et al. Isolation of potent SARS-CoV-2 neutralizing antibodies and protection from disease in a small animal model. *Science* **2020**, *369*, 956−963.
(34) Labzin, L. I.; Chew, K. Y.; Eschke, K.; Wang, X. H.; Esposito, T.; Stocks, C. J.; Rae, J.; Patrick, R.; Mostafavi, H.; Hill, B.; et al. Macrophage ACE2 is necessary for SARS-CoV-2 replication and subsequent cytokine responses that restrict continued virion release. *Sci. Signal.* **2023**, *16*, No. eabq1366.
(35) Cong, B. Y.; Dong, X.; Yang, Z. H.; Yu, P.; Chai, Y. Y.; Liu, J. Q.; Zhang, M. H.; Zang, Y. P.; Kang, J. M.; Feng, Y.; et al. Single-cell spatiotemporal analysis of the lungs reveals *Slamf* $^{9+}$ macrophages involved in viral clearance and inflammation resolution. *Cell Discovery* **2024**, *10*, 104.
(36) Wang, Z. Z.; Popowski, K. D.; Zhu, D. S.; Abad, B. L. D.; Wang, X. Y.; Liu, M. R.; Lutz, H.; De Naeyer, N.; DeMarco, C. T.; Denny, T. N.; et al. Exosomes decorated with a recombinant SARS-CoV-2 receptor-binding domain as an inhalable COVID-19 vaccine. *Nat. Biomed. Eng.* **2022**, *6*, 791−805.
(37) Wang, L.; Wang, X. Y.; Yang, F. M.; Liu, Y.; Meng, L.; Pang, Y.; Zhang, M. M.; Chen, F. J.; Pan, C.; Lin, S. S.; et al. Systemic antiviral immunization by virus-mimicking nanoparticles- decorated erythrocytes. *Nano Today* **2021**, *40*, 101280.
(38) Lin, H.; Yang, C.; Luo, Y.; Ge, M.; Shen, H.; Zhang, X. L.; Shi, J. L. Biomimetic Nanomedicine-Triggered *in situ* Vaccination for Innate and Adaptive Immunity Activations for Bacterial Osteomyelitis Treatment. *ACS Nano* **2022**, *16*, 5943−5960.


https://doi.org/10.1021/acs.nanolett.4c04653
*Nano Lett.* 2024, 24, 15136−15141